Published OnlineFirst November 25, 2014; DOI: 10.1158/0008-5472.CAN-14-1337

Cancer Research

Nitric Oxide Mediates Metabolic Coupling of Omentum-Derived Adipose Stroma to Ovarian and Endometrial Cancer Cells

Bahar Salimian Rizi[1], Christine Caneba[2], Aleksandra Nowicka[3], Ahmad W. Nabiyar[4], Xinran Liu[1], Kevin Chen[2], Ann Klopp[3], and Deepak Nagrath[1,2]

Abstract

Omental adipose stromal cells (O-ASC) are a multipotent population of mesenchymal stem cells contained in the omentum tissue that promote endometrial and ovarian tumor proliferation, migration, and drug resistance. The mechanistic underpinnings of O-ASCs' role in tumor progression and growth are unclear. Here, we propose a novel nitric oxide (NO)–mediated metabolic coupling between O-ASCs and gynecologic cancer cells in which O-ASCs support NO homeostasis in malignant cells. NO is synthesized endogenously by the conversion of L-arginine into citrulline through nitric oxide synthase (NOS). Through arginine depletion in the media using L-arginase and NOS inhibition in cancer cells using N^G-nitro-L-arginine methyl ester (L-NAME), we demonstrate that patient-derived O-ASCs increase NO levels in ovarian and endometrial cancer cells and promote proliferation in these cells. O-ASCs and cancer cell cocultures revealed that cancer cells use O-ASC–secreted arginine and in turn secrete citrulline in the microenvironment. Interestingly, citrulline increased adipogenesis potential of the O-ASCs. Furthermore, we found that O-ASCs increased NO synthesis in cancer cells, leading to decrease in mitochondrial respiration in these cells. Our findings suggest that O-ASCs upregulate glycolysis and reduce oxidative stress in cancer cells by increasing NO levels through paracrine metabolite secretion. Significantly, we found that O-ASC–mediated chemoresistance in cancer cells can be deregulated by altering NO homeostasis. A combined approach of targeting secreted arginine through L-arginase, along with targeting microenvironment-secreted factors using L-NAME, may be a viable therapeutic approach for targeting ovarian and endometrial cancers. *Cancer Res; 75(2); 1–16. ©2014 AACR.*

Introduction

The omentum, the fatty pad of adipose tissue that covers the bowel, is a frequent site of metastasis for ovarian cancer (1–3). The omentum contains a population of stromal cells, adipose stromal cells (ASC), which are multipotent mesenchymal stem cells that engraft in tumors and can support cancer progression (4–7). Omentum-derived ASCs (O-ASC) may contribute to the formation of a hospitable environment for the development of ovarian cancer metastasis (8, 9). Recently, we showed that O-ASCs promoted proliferation, migration, chemotherapy, and radiation response of ovarian cancer cells (8). Furthermore, O-ASCs recruited to tumors expressed factors that enhanced tumor vascularization, promoted survival, and proliferation of endometrial cancer cells (9). However, the mechanism by which O-ASCs regulate tumor growth and induce chemoresistance is unknown. We hypothesize that "nitric oxide homeostasis" is a key player in regulating reciprocal communication between O-ASCs and gynecologic cancers (ovarian cancer and endometrial cancer).

O-ASCs can differentiate into adipocytes lineage, promote tumor initiation, growth, vascularization, metastasis, and resistance to chemotherapy in many tumor models (2, 10). Recently, we showed that O-ASCs promoted proliferation, migration, chemotherapy, and radiation response of ovarian cancer cells (8). Omentum has been shown to promote colonization of ovarian cancer cells (11). Mounting evidence suggests that bidirectional communication between ovarian cancer and its microenvironment is critical for tumor growth (12). One critically important, yet often overlooked, contributor to ovarian cancer and endometrial cancer tumor growth, progression, and metastasis to omentum is nitric oxide (NO). Cancer cells' high affinity for NO could explain the proximity of many carcinomas to fatty tissue, and thus the high positive correlation between obesity and cancer (13).

NO is an intracellular signaling molecule that plays pleiotropic roles in cellular physiology and diseases (14) by regulating cellular levels of pH, blood flow, oxygen, and nutrients (15). NO is synthesized endogenously by the conversion of L-arginine into citrulline through nitric oxide synthase (NOS). NOS is differentially expressed in obese and nonobese individuals and is overexpressed in many tumors (16, 17). It has been shown that high levels of NOS activity exist in malignant tissue from gynecologic cancers (18) and higher NOS expressions were correlated to the

[1]Department of Chemical and Biomolecular Engineering, Rice University, Houston, Texas. [2]Department of Bioengineering, Rice University, Houston, Texas. [3]University of Texas, MD Anderson Cancer Center, Houston, Texas. [4]GE Power & Water, Boulder, Colorado.

Note: Supplementary data for this article are available at Cancer Research Online (http://cancerres.aacrjournals.org/).

Corresponding Author: Deepak Nagrath, Department of Chemical and Biomolecular Engineering, MS-362, Rice University, 6100 Main Street, Houston, TX 77005. Phone: 713-348-6408; Fax: 713-348-5478; E-mail: deepak.nagrath@rice.edu

doi: 10.1158/0008-5472.CAN-14-1337

Published OnlineFirst November 25, 2014; DOI: 10.1158/0008-5472.CAN-14-1337

more advanced stages of breast cancers (19). NO acts in a bimodal manner in cancer research, at low concentrations it increases proliferation, angiogenesis, invasiveness, metastasis, and cytoprotection (10, 20, 21). However, high concentrations of NO induce extensive DNA damage, oxidative, and nitrosative stress that lead to cytotoxicity and apoptosis of tumor cells (22, 23). The impact of altering NO metabolism in the tumor microenvironment is unknown.

Altered cancer cells' metabolism is one of the tumor hallmarks (24). Warburg reported that cancer cells rely on glycolysis for their energetic needs even under aerobic conditions. Despite glycolysis being an inefficient mechanism for ATP production compared with mitochondrial tricarboxylic acid (TCA) cycle, cancer cells were found to be metabolically reprogrammed for increased glucose uptake and they route the intermediate metabolite pyruvate toward lactate secretion. Treating cancer as an isolated epithelial cell disease has not been successful because of the unique interplay between the various aspects of the tumor and microenvironment (25). Thus, the microenvironment has been the recent target of molecular strategies for tumor treatment (12). Little is known about the features of metabolic alterations induced by O-ASCs in cancer cells. We hypothesize that O-ASCs regulate NO metabolism in ovarian cancer and endometrial cancer cells, thereby support tumor growth, survival, and chemoresistance. We propose a previously unexplored metabolic coupling among ovarian cancer, endometrial cancer cells, and O-ASCs by showing that O-ASCs affect cancer hallmarks by altering the NO homeostasis. Furthermore, we demonstrate that patient-derived O-ASCs regulate NO homeostasis in ovarian cancer and endometrial cancer cells and promote tumor growth and induce chemoresistance in these cancer cells. Collectively, our study will lead to significant advances in the understanding of the omentum in altering cancer metabolism and lead to novel therapeutics, enabling treatment disrupting the communication between the tumor and omentum.

Materials and Methods

Isolation of patient-derived O-ASC

Grossly normal-appearing human omentum was obtained according to Institutional Review Board–approved protocols. O-ASCs were isolated as described in previously published protocol (8). Informed consent for tissue banking was obtained from each patient. All clinical investigations were conducted according to the principles expressed in the Declaration of Helsinki. Written consent was obtained from each patient. O-ASCs were classified as lean (BMI$\leq$25) and overweight (BMI>25). ASCs were isolated according to published protocols (24). After isolation, cells were expanded *in vitro*, and then characterized with flow cytometry to evaluate cell-surface marker expression. O-ASCs were characterized with antibodies against the following markers: CD34, CD44, CD45, CD29, CD90, EpCam (from Becton Dickinson), and CD105 (from BioLegend).

Cells and reagents

The human ovarian and endometrial carcinoma cell lines, OVCAR429 and HEC-1-A, were grown in RPMI-1640 containing 10% fetal bovine serum and 2% penicillin and streptomycin mixture. O-ASCs were maintained in MEM-α containing 20% fetal bovine serum and 1% penicillin and streptomycin. All cells were kept at 37°C in a humidified atmosphere of 5% CO_2. N^G-nitro-L-arginine methyl ester (L-NAME) and SNAP were purchased from Enzo Life Sciences. L-arginase from bovine was obtained from Sigma-Aldrich.

Direct and indirect coculture

For indirect cocultures, transwell plates (Corning) with two compartments separated by a polycarbonate membrane with 0.4-μm pores were used. O-ASCs were seeded in the upper compartment (0.2×10^5 cells/well) and cancer cells in the lower compartment (1×10^5 cells/well). O-ASCs and cancer cells could not contact each other directly although they can communicate through the soluble factors derived from each cell type such as metabolites and growth factors. The cells were cocultured for 2 to 5 days, depending on experiments. Cancer cells and O-ASCs alone were cultured as controls.

For direct coculture, O-ASCs were seeded in 96-well microplates and incubated at 37°C until they attached to surface. Next, cancer cells were seeded on top of attached O-ASCS. The ratio of O-ASCs to cancer cells was 3:1.

Quantitative analysis of NO

Cancer cells either experienced transwell coculture of O-ASCs or they were monocultured for 72 hours. The media were replaced with fresh media (RPMI-1640) 3 hours before sample collection. For measurement of NO content in homogenates, cells were washed in PBS solution at 4°C and lysed in PBS solution containing 1% Nonidet *P*-40, 2 mmol/L N-ethylmaleimide, 0.2 mmol/L diethylenetriaminepentaacetic dianhydride, and protease inhibitors. After three instant freeze–thaw cycles (−80/37°C), lysates were passed through a 29-gauge needle to reduce viscosity and spun at $2{,}000 \times g$ for 10 minutes at 4°C. Protein concentration was measured to normalize the NO results. Samples were assessed by using a Sievers NO analyzer (280i; GE Analytical Instruments).

Cell viability analysis

OVCAR429 and HEC-1-A were cocultured either directly or indirectly with O-ASCs at 37°C for 2 to 5 days, depending on the experiment. For indirect coculture, cancer cells were trypsinized and stained with Trypan Blue. Viable cancer cells were quantified by hemocytometer counting. For direct coculture experiments, OVCAR429 and HEC-1-A cells stably transfected with firefly luciferase gene using a lentiviral method were used. Cancer cells' viability and proliferation was determined by measuring luminescence by a plate reader (SpectraMax M5; Molecular Devices).

UPLC

Cell supernatants were collected after 24 hours of incubation with fresh media and were stored at −80°C until further analysis. Extracellular metabolite profiling was performed using a Waters ACQUITY ultra-performance liquid chromatography (UPLC) system. Derivatization of samples was according to the manufacturer's instructions. Briefly, deproteinized samples are prepared by mixing 1:1 ratio of collected media with 10% sulfosalicylic acid/norvaline solution. The mixture is centrifuged for no more than 5 minutes at a fixed angle at 13,000 rpm. Supernatant from the centrifugation is then added to borate buffer/NaOH mixture along with reconstituted MassTrak AAA regent. Chromatographic separations were performed on a 2.1 mm $\times$ 150 mm chromatography column. The column was maintained at 43°C, eluted with a mix of 99.9% of MassTrak AAA eluent A concentrate (8%–10% acetonitrile, 4%–6% formic acid, 84%–88% ammonium acetate/water solution), and diluted at 10% in miliQ water and 0.1% of MassTrak AAA eluent B ($\geq$95% acetonitrile, $\leq$5% acetic

Published OnlineFirst November 25, 2014; DOI: 10.1158/0008-5472.CAN-14-1337

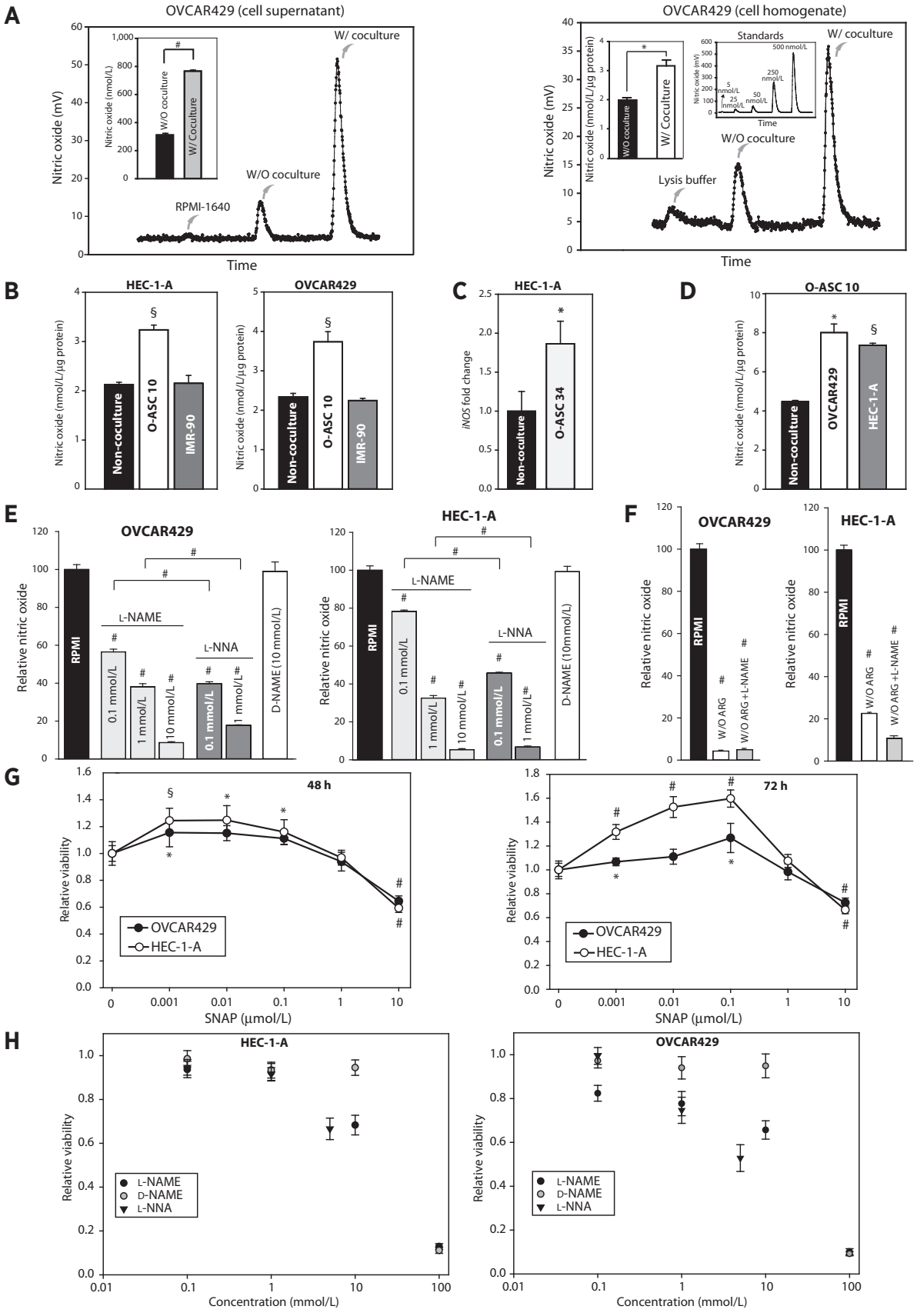

Published OnlineFirst November 25, 2014; DOI: 10.1158/0008-5472.CAN-14-1337

acid) with a MassTrak AAA eluent B (≥95% acetonitrile, ≤5% acetic acid derivatized sample was injected into the column with UV detection at 260 nm.

Adipogenesis

O-ASCs were cultured in a 12-well plate in MEM-α media until cells were almost confluent. The media were replaced with quick differentiation media that includes DMEM/F12, human transferrin (10 μg/mL), insulin (0.02 μmol/L), cortisol (0.1 μmol/L), rosiglitazone (1 μmol/L), dexamethasone (1 μmol/L), IBMX (500 μmol/L), and indomethacine (200 μmol/L; all were purchased from Sigma-Aldrich). After 4 days, the media were changed to adipogenic media including insulin (0.02 μmol/L) and rosiglitazone (1 μmol/L). Differentiation of O-ASCs was determined by either OilRed O staining or measuring glycerol 3-phosphate dehydrogenase (G3PDH) activity.

OilRed O staining

The cells incubated in adipogenic media for 7 or 14 days (depending on the experiment) were rinsed twice with warm PBS. The cells were fixed with 5 vol% glutaraldehyde solution in PBS for 20 minutes at room temperature. The oil red O solution was prepared by mixing an oil red O (0.3 wt%) stock solution in isopropanol (6 mL) and 4-mL distilled water followed by the filtration through Whatman filter (No. 1). Fixed cells were incubated with oil red O for 10 minutes at room temperature. The cells were rinsed with tap water to be viewed by phase-contrast microscopy (EVOS XL Core Cell Imaging System).

G3PDH activity

O-ASCs were grown and induced to differentiate in 12-well plate as describe above. The G3PDH activity was measured using the method by Sottile and Seuwen (26). Briefly, the media were removed and the cells were washed once with PBS. An ice-cold homogenization solution was then added (20 mmol/L Tris, 1 mmol/L EDTA, 1 mmol/L β-mercaptoethanol, and pH adjusted to 7.3). Cell lysate was stored at −20°C until measurement. To prepare the enzyme reaction, 80 μL of reaction mix (0.1 mol/L triethanolamine, 2.5 mmol/L EDTA, 0.1 mmol/L β-mercaptoethanol, 334 mmol/L NADH, and pH adjusted to 7.7) and 10 μL of cell lysate were added to each well, and plates were preincubated for 10 minutes at 37°C. Dihydroxyacetone phosphate (DHAP) was added to start the reaction (10 μL/well of a 4 mmol/L stock solution in H_2O). Absorbance (340 nmol/L) was monitored at time intervals by a plate reader (SpectraMax M5; Molecular Devices). The protein content of cell cultures was determined in parallel wells. Results are expressed as mUI/mg protein (1 U = 1 μmol NADH/min). For control experiments, G3PDH from human was used (Abcam).

XF bioenergetics assay

Mitochondrial oxygen consumption was measured with an XF24 Extracellular Flux Analyzer (Seahorse Bioscience). Cancer cells were reseeded upon termination of indirect coculture with O-ASCs in Seahorse 24-well microplates at a cell density of 0.5×10^5 cells per well. The plate is incubated at 37°C with 5% CO_2 until cells were attached to surface. The attached cells were washed with 200 μL of assay media (FBS excluded RPMI) and were incubated at 37°C without CO_2 for 1 hour for equilibrium. The endogenous respiration or basal oxygen consumption rate (OCR) was then measured. The endogenous coupling degree of the OXPHOS system was assessed using oligomycin (2 μg/mL), an inhibitor of the F_1F_0-ATPsynthase. The uncoupled OCR was also measured in the presence of 1 μmol/L of FCCP. Finally, the cells were treated with a mitochondrial complex I inhibitor, rotenone (2.5 μmol/L), to assess the mitochondrial contribution to OCR.

Metabolic assays

The lactate secretion was quantified with the lactate kit (Trinity Biotech). The lactate secreted into the growth media by the cells after 24 hours of incubation was measured according to the manufacturer's instructions. The absorbance at 540 nm was proportional to the lactate concentration in the sample. The results were expressed in μmol/million cells. By a similar method, the glucose consumption was determined with the Glucose Auto-kit (Wako).

The pyruvate uptake was estimated spectrophotometrically by measuring the remaining pyruvate in growth media after 24 hours of incubation of the cells in different experimental conditions as specified in the text. The aim of this assay was to determine the amount of NADH oxidized at 340 nm in a 96-well plate format. Each well contained 20 μL of sample, NADH reagent, and lactate dehydrogenase reconstituted at 50% in glycerol and diluted to 1:20 in Tris (0.1 mol/L; pH 7).

ATP measurements

The intracellular ATP content was measured using the CellTiter-Glo Luminescent Cell Viability Assay (Promega). The cells were seeded in 96-well plates upon termination of transwell coculture at 0.5×10^5 cells per well and incubated at 37°C with 5% CO_2 until cells are attached to surface. Next, cells were incubated for 3 hours in the absence or the presence of oligomycin (2 μg/mL) and 2-deoxyglucose (100 mmol/L) at 37°C. The ATP content was

Figure 1.

O-ASCs induce NO synthesis of ovarian cancers and endometrial cancers. A, OVCAR429 cells were transwell cocultured with O-ASC 35 for 3 days. The media were replaced with fresh RPMI media 3 hours before sample collection. NO content was assessed in the samples (cell homogenate and cell supernatant) using Sievers NO analyzer. Protein content of samples was used for normalization of data. B, cancer cells were transwell cocultured with either O-ASC 10 or IMR-90 before NO content was measured in cancer cell homogenate samples. C, iNOS mRNA expression of HEC-1-A was measured after 4 days of transwell coculture with O-ASC 34. D, NO content in O-ASC 10 was measured upon its transwell coculture with OVCAR429 and HEC-1-A for 3 days. O-ASC 10 cell homogenate was used for NO analysis. E, cancer cells were treated with NOS inhibitors for 48 hours before NO measurements in cell homogenates. F, OVCAR429 and HEC-1-A were cultured with either complete RPMI or arginine-free media for 48 hours. L-NAME (10 mmol/L) was added to inhibit endogenous NO synthesis. G, cancer cells were treated with varying concentrations of SNAP and viability of cells was measured. H, cells were treated with NO inhibitors for 48 hours before their viability was measured. Data are expressed as mean ± SE; $n > 6$. *, $P < 0.05$; §, $P < 0.01$; and #, $P < 0.001$. A *t* test was used for single comparisons. Multiple comparisons versus a control group were analyzed by the Dunnett method. All pairwise multiple comparisons were analyzed by the Bonferroni test to compare lean and overweight patients' samples.

Published OnlineFirst November 25, 2014; DOI: 10.1158/0008-5472.CAN-14-1337

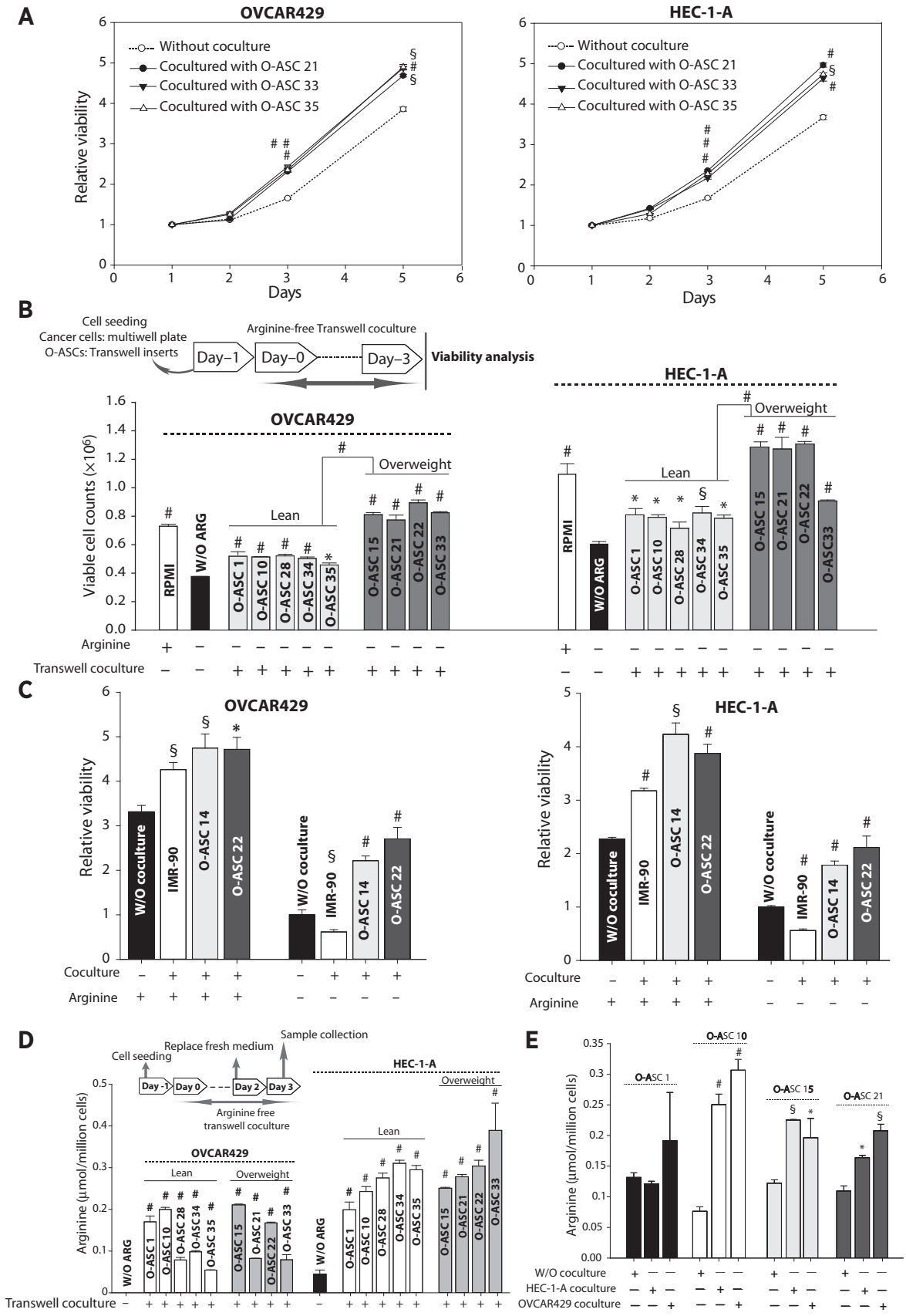

Published OnlineFirst November 25, 2014; DOI: 10.1158/0008-5472.CAN-14-1337

thereby measured according to the manufacturer's instructions, with a spectrophotometer SpectraMax M5 (Molecular Devices).

Detection of intracellular reactive oxygen species

The generation of reactive oxygen species (ROS) was determined using the ROS-specific fluorescent dye H2DCF-DA. Briefly, cancer cells and O-ASCs were transwell cocultured for 3 days. Cancer cells were trypsinized and re-plated in 96-well plates until cells were attached to surface. Next, cells were washed with PBS and incubated with 10 μmol/L H2DCF-DA for 20 minutes at 37°C. The probe was washed by PBS and the DCF fluorescence (Ex 485 nm and Em 535 nm) was measured by a plate reader (SpectraMax M5; Molecular Devices).

NADPH measurement

A water-soluble tetrazolium salt was used to monitor the amount of nicotinamide adenine dinucleotide phosphate (NADPH) in cancer cells through its reduction to a yellow colored water-soluble formazan dye. Briefly, cells were washed with PBS and 100 μL of XTT/1-methoxyPMS solution (251 and 0.5 mmol/L, respectively) was added in each well. Formazan formation was quantified by measuring absorbance at 650 nm using a plate reader (SpectraMax M5; Molecular Devices).

Analysis of gene expression using real-time PCR

Cells from transwell coculture and monoculture were used. Total RNA was isolated using an RNeasy mini kit (Qiagen). cDNA was synthesized from 1.0 μg of total RNA with the High Capacity cDNA Reverse Transcription Kit (Applied Biosystems) using a Veriti 96-well Thermal Cycler (Applied Biosystems). The mRNA levels of gene of interest were examined by real-time PCR using 50 ng of the resultant cDNA. Real-time PCR was performed with the SYBR Green PCR Master Mix (Applied Biosystems) using the StepOnePlus Real-Time PCR System (Applied Biosystems). The reactions with gene of interest were normalized against glyceraldehyde-3-phosphate dehydrogenase (GAPDH). Specific primer sets were as follows listed 5′–3′; forward and reverse, respectively): *iNOS*, AGATAAGTGACATAAGTGACC and CATTCTGCTGCTTGCTGAG; *AP2*, GCATGGCCAAACCTAACATGA and CCTGGCCCAGTATGAAGGAAA; and *LPL*, CTGGACGGTAACAGGAATGTATGAG and CATCAGGAGAAAGACGACTCGG. Reactions were performed in a volume of 20 μL.

Data analysis

Results are expressed as mean ± SEM of at least triplicates. Statistical analyses were performed for multiple comparisons with one-way ANOVA with Dunnett post hoc tests and Bonferroni. The Student *t* test was implemented for two comparison analyses. Differences were considered statically significant at $P < 0.05$ (*, $P < 0.05$; §, $P < 0.01$; and #, $P < 0.001$).

Results

O-ASCs induce NO synthesis in ovarian cancers and endometrial cancers

We hypothesized that "NO homeostasis" is a key player in regulating reciprocal communication between O-ASCs and cancer cells. We tested NO levels in coculture media supernatants of O-ASCs and ovarian cancer cells (Fig. 1A) as compared with tumor cells cultured alone. Significantly higher NO was detected in cocultures. To further confirm the increased NO levels in cancer cells, we measured NO in cancer cell homogenates. Indeed, NO levels were higher in cell homogenates of cancer cells that were in cocultures compared with cancer cells cultured alone (Fig. 1A). Interestingly, control cell line (IMR-90, human fibroblasts) was unable to increase NO synthesis in cocultures (Fig. 1B). These results suggest that O-ASCs selectively increase NO synthesis in cancer cells. Furthermore, O-ASCs increased expression of *iNOS* in HEC-1-A cells in Transwell cocultures (Fig. 1C). Cancer cells in turn increased NO synthesis in O-ASCs; O-ASCs synthesized higher NO when transwell cocultured with ovarian cancer and endometrial cancer cells (Fig. 1D).

To confirm that NO synthesis in these cells is by conversion of arginine into citrulline through NOS, we measured NO levels in the presence of NOS inhibitor L-NAME (Fig. 1E). As seen in Fig. 1E, L-NAME reduced the NO production in a dose-dependent manner in cancer cells. The hydrolysis of L-NAME results in L-NNA, a fully functional inhibitor of NOS. L-NAME action on NOS was further confirmed using L-NNA, an active form of the NOS inhibitor. Furthermore, D-NAME, an inactive enantiomer of L-NAME that served as negative control, was ineffective in reducing the NO production in cancer cells. To ascertain whether arginine is a major source for NO synthesis in these cells, we measured NO synthesis under arginine depletion conditions with and without L-NAME. As see in Fig. 1F, under arginine-deprived conditions, NO synthesis is drastically reduced, thus indicating that other nutrients contribution toward NO synthesis is negligible. Moreover, when L-NAME is added to inhibit NO production through endogenously synthesized arginine, the decrease of NO levels was not significant. To confirm whether arginine levels in cancer cells were regulated through arginase, an enzyme that converts arginine into ornithine and urea, we measured urea secretion in these cells. Our

Figure 2.

O-ASCs positively regulate ovarian cancers and endometrial cancer growth through arginine. A, O-ASCs and stably luciferase transfected ovarian cancer and endometrial cancer cells were in contact cocultures in 96-well plate. Luciferin (150 μg/mL) was added and luminescence was assessed to quantify viable cells for 5 days. The media were changed to RPMI after each measurement for further viability assessment. B, OVCAR429 and HEC-1-A cells were seeded in 6-well plates, while O-ASCs were seeded on top of transwell inserts. The media were changed to RPMI without arginine during 3 days of indirect coculture. Cancer cells' viability was measured and was reported in million units. Cancer cells without cocultures are shown in white (medium with arginine) and black (medium without arginine) bars. Cocultured cancer cells (both OVCAR42 and HEC-1-A) are labeled according to the O-ASCs they were cocultured. Cancer cells without coculture and without arginine were used as the control. C, cancer cells were cocultured in direct contact either with O-ASCs or IMR-90 for 3 days before their viability was measured. The coculture media were complete RPMI or RPMI without arginine. Cancer cells without coculture were used as the control. D, arginine contents of cancer cells and O-ASCs in mono and coculture, respectively. OVCAR429 and HEC-1-A were transwell cocultured with O-ASCs for 3 days in arginine-free media. Fresh media were replaced 24 hours before sample collection. Arginine contents of collected samples were analyzed by UPLC. E, O-ASCs from transwell coculture were separated and incubated with arginine-free media for 24 hours before the sample collection. Arginine contents of the spent media were measured by UPLC. Data are expressed as mean ± SE; $n > 6$. *, $P < 0.05$; §, $P < 0.01$; and #, $P < 0.001$. A *t* test was used for single comparisons. Multiple comparisons versus a control group were analyzed by the Dunnett method. All pairwise multiple comparisons were analyzed by the Bonferroni test to compare lean and overweight patients' samples.

Published OnlineFirst November 25, 2014; DOI: 10.1158/0008-5472.CAN-14-1337

results show that cancer cells have negligible arginase activity as measured through urea secreted in the medium (Supplementary Fig. S1A). Furthermore, gene expression analysis using the Oncomine database (27) showed that arginase-1 (ARG1) expression in ovarian and endometrial cancers was similar to normal ovarian epithelium (Supplementary Fig. S1B). The urea secretion data were in line with The Cancer Genome Atlas (TCGA) data that did not show any upregulation of arginase gene expression (ARG1) in cancer cells.

We next sought to determine whether NO regulates cancer proliferation. We used S-nitroso-N-acetyl-DL-penicillamine (SNAP), a NO donor, with varying concentrations to investigate NO's effect on cancer cell growth under complete media conditions. Our results illustrate that SNAP plays a bimodal role in the growth of ovarian cancers and endometrial cancers. At low concentrations of SNAP (less than 0.1 μmol/L), increased growth of cancer cells (Fig. 1G), whereas higher concentrations of SNAP (greater than 1 μmol/L) have cytotoxic effects. To confirm NO's role in increasing proliferation, we used low to high concentrations of L-NAME. As seen in Fig. 1H, L-NAME and L-NNA had similar behavior at low concentrations (<1 mmol/L) where they marginally reduced viability. On the contrary, both L-NNA and L-NAME significantly reduced viability at 10 mmol/L concentration compared with D-NAME control.

O-ASCs positively regulate ovarian cancer and endometrial cancer cells growth through arginine

To understand O-ASCs' role in regulating cancer cells growth, we first cultured ovarian cancers and endometrial cancers cells with and without O-ASCs cocultures for 5 days (Fig. 2A). O-ASCs increased the proliferation of both endometrial (HEC-1-A) and ovarian (OVCAR429) cancer cell lines. Next, to elucidate a precise role for the NO pathway in O-ASC–induced tumor pathogenesis, we cocultured ovarian cancer and endometrial cancer cells under complete media and arginine-deprived conditions (Fig. 2B). Cells cultured under arginine-deprived conditions will have reduced NO synthesis. We found that ovarian cancer and endometrial cancer cells are arginine-dependent and hence had reduced proliferation. Significantly, transwell cocultures of both overweight and lean O-ASCs with HEC-1-A and OVCAR429 cells rescued the proliferation rate in these cells under arginine-deprivation conditions. Interestingly, the rescue of proliferation was higher when cancer cells were cocultured with overweight O-ASCs compared with their lean counterparts. Similar results were obtained when cancer cells were cultured in conditioned media obtained from lean and overweight O-ASCs (Supplementary Fig. S2A). As seen in the figure, the rescue effect with conditioned media for both lean and overweight O-ASCs is less pronounced compared with rescue of proliferation obtained with transwell cocultures. We further confirmed the effect of O-ASCs in rescuing proliferation under arginine-deprivation conditions under direct contact cocultures (Fig. 2C). Interestingly, control cell line was ineffective in rescuing the reduced proliferation in cancer cells under arginine-deprivation conditions. In line with these findings, IMR-90 was found to be arginine-dependent for proliferation (Supplementary Fig. S2B). This is in contrast to complete media conditions where IMR-90 cells did increase proliferation of cancer cells.

To establish whether the O-ASC–mediated rescue under arginine deprivation is through the secreted arginine, we measured arginine using UPLC in spent media of transwell cocultures of O-ASCs and cancer cells under arginine-deprivation conditions (Fig. 2D). As seen in the figure, both lean and overweight O-ASCs had significant arginine secretion in coculture with both ovarian and endometrial cancer cells, while tumor cells alone did not secrete arginine. Interestingly, cancer cells exhibited reciprocal effect by increasing arginine synthesis from O-ASCs (Fig. 2E). As seen in the figure, arginine secretion from O-ASCs is higher when they were cocultured with cancer cells.

Inhibition of endogenous NO synthesis abrogates elevated viability of cancer cells induced by O-ASCs

The above experiments demonstrated that O-ASC coculture rescued the growth-inhibitory effect of arginine depletion. We further investigated whether O-ASCs secrete arginine, an essential metabolite for NO synthesis, or they secrete factors that upregulate NO synthesis in cancer cells. To assess whether O-ASCs secrete arginine under arginine-deprivation conditions, we added L-arginase, an enzyme that converts arginine to ornithine and urea, in direct cocultures of O-ASCs and cancer cells seeded in a ratio of 3:1. We first evaluated the efficacy of arginase in depleting arginine in the medium (Supplementary Fig. S3). As seen in the figure, arginine levels decreased with increasing arginase concentration. The L-arginase treatment depletes secreted arginine and thereby disrupts the rescue effect of O-ASCs. Indeed, L-arginase (10 U/mL) disrupted the rescue potential of O-ASCs, thus suggesting that O-ASCs secreted arginine is the possible cause behind the rescue potential of O-ASCs (Fig. 3A and B). We added L-NAME in contact cocultures and monocultures under arginine-deprivation conditions to determine whether NO signaling is required for the O-ASC effect on cancer cell proliferation (Fig. 3C and D). Consistent with L-arginase results, the addition of L-NAME decreased the rescue effect of O-ASCs on cancer cells' proliferation in cocultures, thereby suggesting that O-ASCs effects on cancer cell proliferation are mediated by NO signaling. Interestingly, overweight O-ASCs had stronger rescue effect in cocultures for both ovarian and endometrial cancer cells. To determine whether the O-ASCs effect on cancer cell proliferation is mediated by secreted factors, we added L-NAME to transwell cocultures (Fig. 3E and F). In agreement with L-arginase results, L-NAME addition significantly reduced proliferation in cocultures. To further demonstrate the direct involvement of the NO pathway in rescue of cancer cells growth, we added SNAP (100 nmol/L), a NO donor, under arginine-deprivation and NOS-inhibition conditions (using L-NAME; Fig. 3G). Remarkably, SNAP rescued the reduced proliferation of cancer cells under both conditions and the rescue effect was similar to O-ASC–induced rescue of cancer cell growth under L-NAME and arginine-deprivation conditions.

Citrulline induces adipogenesis of O-ASCs

Cells with high NOS activity convert arginine into citrulline and release NO. In our previous study, we found that ovarian cancer cells secreted citrulline, suggesting significant levels of NOS activity. Thus, we measured citrulline in spent media from transwell cocultures. Interestingly, we found high levels of citrulline in cocultures compared with tumor cells alone (Fig. 4A). These results suggest that cancer cells use arginine from the tumor microenvironment and in turn secrete citrulline to alter the tumor microenvironment. To reveal the reciprocity of cancer cells in modulating O-ASCs, we hypothesized that cancer cells secrete

Published OnlineFirst November 25, 2014; DOI: 10.1158/0008-5472.CAN-14-1337

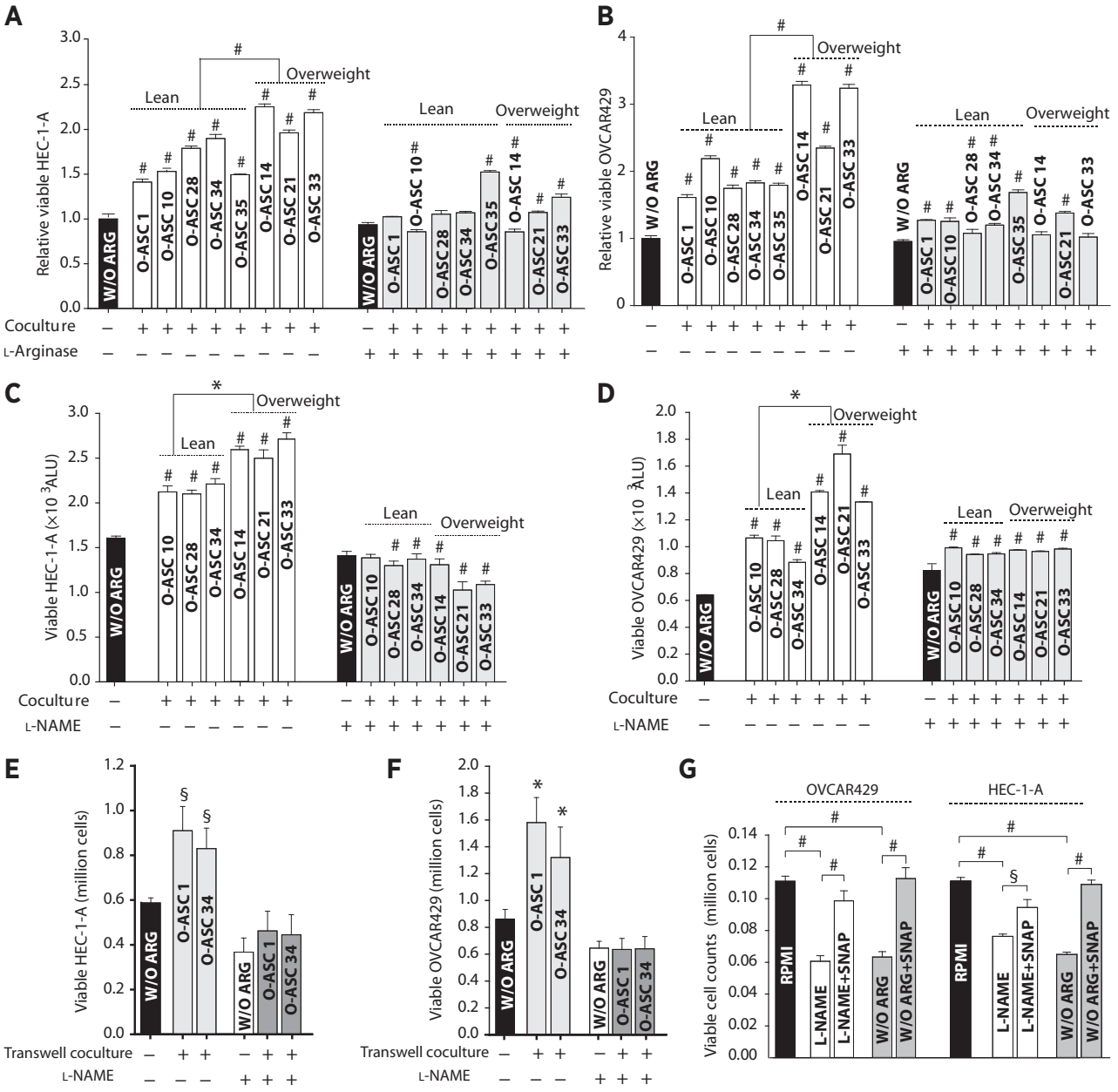

Figure 3.

Inhibition of NO synthesis abrogates elevated viability of cancer cells induced by O-ASCs. A and B, stably luciferase transfected ovarian cancer and endometrial cancer cells (OVCAR429 and HEC-1-A) were cocultured in direct contact with O-ASCs for 3 days (seeding ratio of 1:3). L-arginase (10 U/mL) was added to deplete arginine from media. Luciferin (150 μg/mL) was added to cells and luminescence was assessed to determine viability of cancer cells. Cancer cells without coculture and without L-arginase treatment were used as a control. C and D, L-NAME (20 mmol/L) was added to inhibit NO synthesis by blocking NOS. Cancer cells and O-ASCs were cocultured in direct contact for 72 hours with L-NAME. All the conditions were compared with cancer cells without coculture and without L-NAME treatment. E and F, cancer cells were seeded in 6-well plates while O-ASCs were on top of transwell inserts (the ratio was 1:2, respectively). The media were changed to RPMI without arginine, with and without L-NAME (20 mmol/L), during 3 days of indirect coculture. OVCAR429 and HEC-1-A without coculture and without L-NAME treatment were used as control. G, SNAP (100 nmol/L) and L-NAME (10 mmol/L) were simultaneously added to cancer cells for 48 hours, and the results were compared with the viability of cells treated with L-NAME alone. Moreover, arginine was excluded from the cancer media, and the results were compared with arginine-free media containing SNAP (100 nmol/L). Data are expressed as mean ± SE; $n > 9$. *, $P < 0.05$; §, $P < 0.01$; and #, $P < 0.001$. The Dunnett method was implemented to compare multiple groups versus a control group. Comparisons of lean and obese results were analyzed by the Bonferroni test.

citrulline that could induce adipogenesis. To confirm the hypothesis, we cultured O-ASCs in the presence of citrulline for 48 hours and measured the citrulline content in the spent media using UPLC. Both lean and overweight O-ASCs uptake exogenous citrulline when cultured in the media supplemented with citrulline (Fig. 4B). We monitored the growth rates of O-ASCs in the

Published OnlineFirst November 25, 2014; DOI: 10.1158/0008-5472.CAN-14-1337

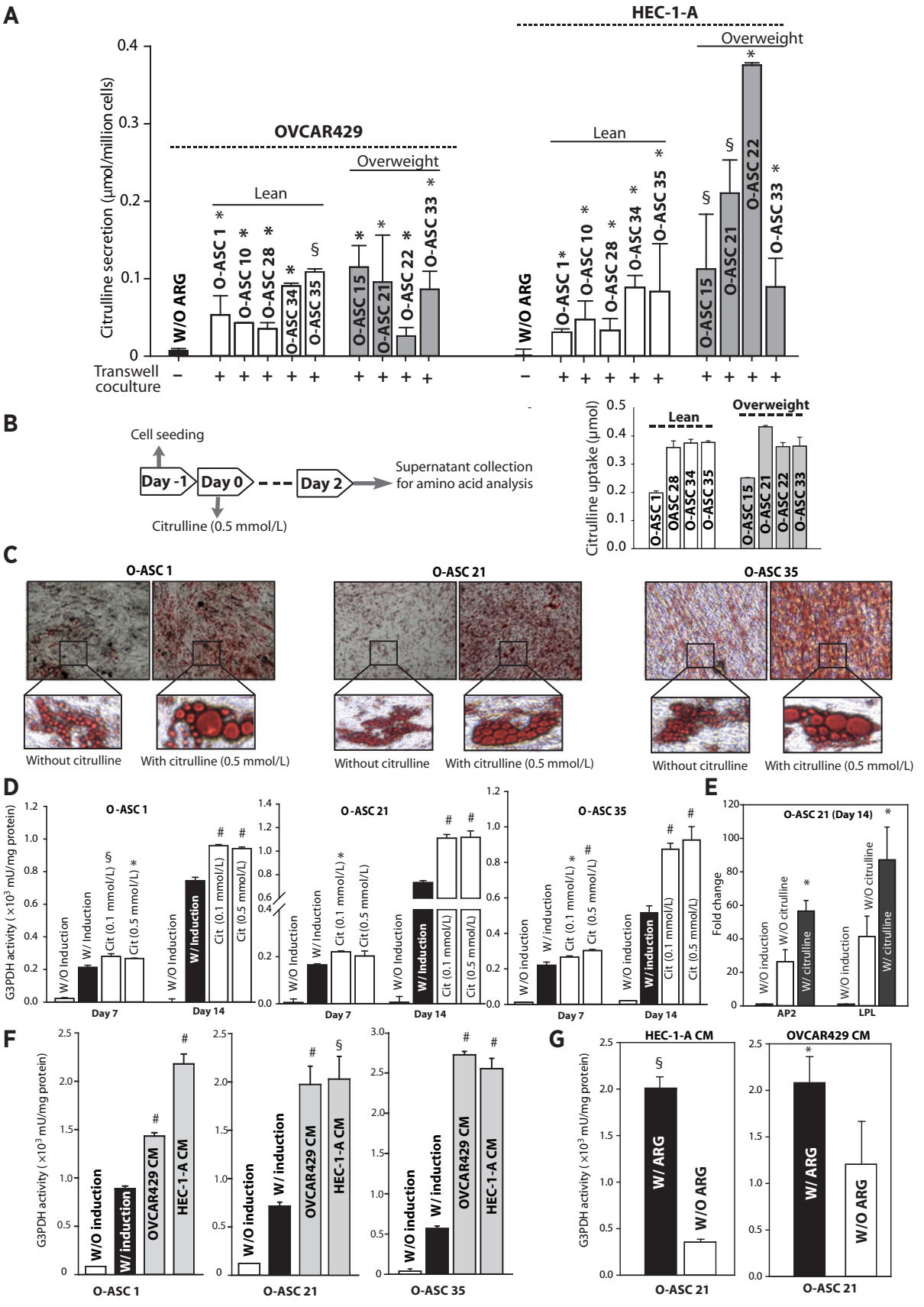

Published OnlineFirst November 25, 2014; DOI: 10.1158/0008-5472.CAN-14-1337

presence of citrulline and no alterations were observed (data not shown).

To confirm our hypothesis, we cultured O-ASCs into adipogenic differentiation media with and without citrulline during the differentiation period. As seen in Fig. 4C, citrulline markedly increased the adipogenic differentiation in the three tested primary patient-derived O-ASC cell lines. The extent of differentiation was similar in lean (O-ASC1, O-ACS 35) and overweight (O-ASC 21) O-ASCs. Noticeably, citrulline increased the size of fat droplets in O-ASCs (Fig. 4C). We further measured the activity of G3PDH, an enzymatic marker for measuring adipogenesis. G3PDH activity is elevated during adipogenesis to support the production of key metabolites such as glycerol. Our results show increased G3PDH activity with citrulline at day 14 of O-ASC differentiation (Fig. 4D). We further measured the mRNA expression of adipocyte protein 2 (AP2) and lipoprotein lipase (LPL) in O-ASCs when adipogenesis was induced with and without citrulline. As seen in Fig. 4E, citrulline increased the expression of these adipogenesis markers. To confirm whether the cancer cells indeed could increase adipogenesis of O-ASCs, we cultured O-ASCs in conditioned media obtained from cancer cells (Fig. 4F). As seen in the figure, conditioned media from cancer cells significantly increased adipogenesis in patient-derived O-ASC cells.

To prove that cancer cells induce adipogenesis via citrulline, we measured adipogenesis using cancer cells' conditioned media with and without arginine. Cancer cells cultured under arginine-deprived conditions will have significantly reduced citrulline in the media. Thus, decreased adipogenesis will be consequent of reduced citrulline in the conditioned media. As seen in Fig. 4G, G3PDH activity of O-ASCs differentiated with was significantly higher for conditioned media with arginine than the conditioned media without arginine. These results confirm our hypothesis that cancer cells increased adipogenesis in O-ASCs and this increase is mediated through secreted citrulline.

O-ASCs modulate cancer cells' mitochondrial bioenergetics

Recently, cancer cells have been found to have altered metabolism and this metabolic rewiring promotes tumor growth and increases malignancy. Previous studies have shown that NO regulates mitochondrial respiration in hepatocytes and cardiomyoctes (28). To elucidate the precise role of O-ASCs in regulating cancer cells' metabolic pathways by altering NO homeostasis, we performed mitochondrial bioenergetic analysis. Our results show that NO reduced respiration of both ovarian cancer and endometrial cancer cells. OCR of cancer cells under arginine-deprived conditions was significantly higher than arginine replete conditions (Fig. 5A). Inhibiting NO synthesis using L-NAME under complete media conditions similarly increased OCR. Furthermore, when SNAP was added OCR drastically decreased. The addition of L-arginine in arginine-free media also decreased OCR, because arginine is a substrate for NO synthesis. These results are consistent with the hypothesis that NO decreases mitochondrial respiration in cancer cells. To determine the effect of O-ASCs on mitochondrial respiration of cancer cells through NO, we measured OCR of cancer cells cocultured with O-ASCs in arginine-deprived condition for 72 hours. We found that cancer cells that were cocultured with both lean and overweight O-ASCs had significantly lower respiration when compared with cancer cells without cocultures (Fig. 5B and C). Furthermore, cancer cells in cocultures with O-ASCs had lower maximal respiratory capacity (measured using FCCP, a protonophoric uncoupler; Fig. 5B). We next measured OCR under NO inhibition conditions. Consistent with previous results, adding L-NAME increased OCR (Fig. 5D). Furthermore, cocultures of both lean and overweight O-ASCs decreased OCR. Thus, from these data, we can conclude that O-ASCs increase NO synthesis in cancer cells, resulting in suppression of mitochondrial respiration in these cells.

O-ASCs regulate ovarian cancers and endometrial cancers' metabolism via NO pathways

To expand our findings on O-ASCs' regulation of cancer cells' metabolism, we examined O-ASCs effect on the glycolysis. NO increased glucose uptake and lactate secretion in cancer cells (Fig. 6A). Both lean and overweight O-ASCs increased glycolysis in cancer cells under coculture conditions in the absence of arginine. These results confirm that O-ASCs induced NO-induced changes consistent with the Warburg effect in these cells. Interestingly, pyruvate uptake was increased in cancer cells cocultured with O-ASCs (Supplementary Fig. S4A). To investigate whether there was reciprocal communication between cancer cells and O-ASCs in regulating metabolism, we measured metabolic activity of O-ASCs with and without cocultures of cancer cells. Interestingly, O-ASCs from cancer cells coculture had higher glucose uptake and lactate secretion (Supplementary Fig. S4B). However, pyruvate uptake was reduced in O-ASCs that were cocultured with cancer cells (Supplementary Fig. S4C). In line with results previously reported, our results suggest that cancer cells transform the microenvironment cells by increasing their glucose metabolism (29). To further confirm NO's regulation of cancer cells' metabolism in

Figure 4.

Citrulline induces adipogenesis of O-ASCs. A, OVCAR429 and HEC-1-A cells were transwell cocultured in arginine-free media for 3 days. Fresh media were replaced 24 hours before sample collection. Citrulline contents of collected samples were analyzed by UPLC. Cancer cell viability was measured and reported in million units to normalize the results. Cancer cells without coculture were used as a control. B, O-ASCs were incubated with MEM-α along with citrulline (0.5 mmol/L) for 48 hours. O-ASCs' supernatant were collected and citrulline content of samples was assessed with UPLC and compared with fresh media at day 0. C, O-ASCs were seeded on a 12-well plate and cultured until confluency. The media were replaced with adipogenic media containing insulin (10 μg/mL), rosiglitazone (2 μmol/L), indomethacin (200 μmol/L), cortisol (100 nmol/L), IBMX (500 μmol/L), and human transferrin (10 μg/mL) with or without citrulline (0.5 mmol/L) for 4 days. Next, the media were exchanged to adipogenic media including only rosiglitazone (2 μmol/L) and insulin (10 μg/mL) with or without citrulline (0.5 mmol/L) for another 10 days. Lipid droplet formation was evaluated with Oil red O staining. The bright field images were taken with ×4 and ×20 magnifications by EVOS XL Core Cell Imaging System. D, G3PDH activity was measured for adipogenic induction with and without citrulline conditions as described in B. E, AP2 and LPL mRNA expressions were measured at day 14 of adipogenic induction in the presence or the absence of citrulline (0.5 mmol/L). F, cancer cells were conditioned 24 hours with MEM-α, and the conditioned media were used to induce adipogenesis in O-ASCs. O-ASCs induced by adipogenic media were used as a control. G, cancer cells were conditioned with either arginine-free or arginine-containing media. Cancer conditioned media without arginine was then replenished with 0.2 g/L-arginine before adipogenic induction. G3PDH activity was measured at day 14 and results from cancer complete conditioned media were compared with arginine-free conditioned media. Data are expressed as mean ± SE; $n > 6$. *, $P < 0.05$; §, $P < 0.01$; and $^{\#}$, $P < 0.001$. A t test was used for single comparisons. The Dunnett method was implemented to compare multiple groups versus a control group.

Published OnlineFirst November 25, 2014; DOI: 10.1158/0008-5472.CAN-14-1337

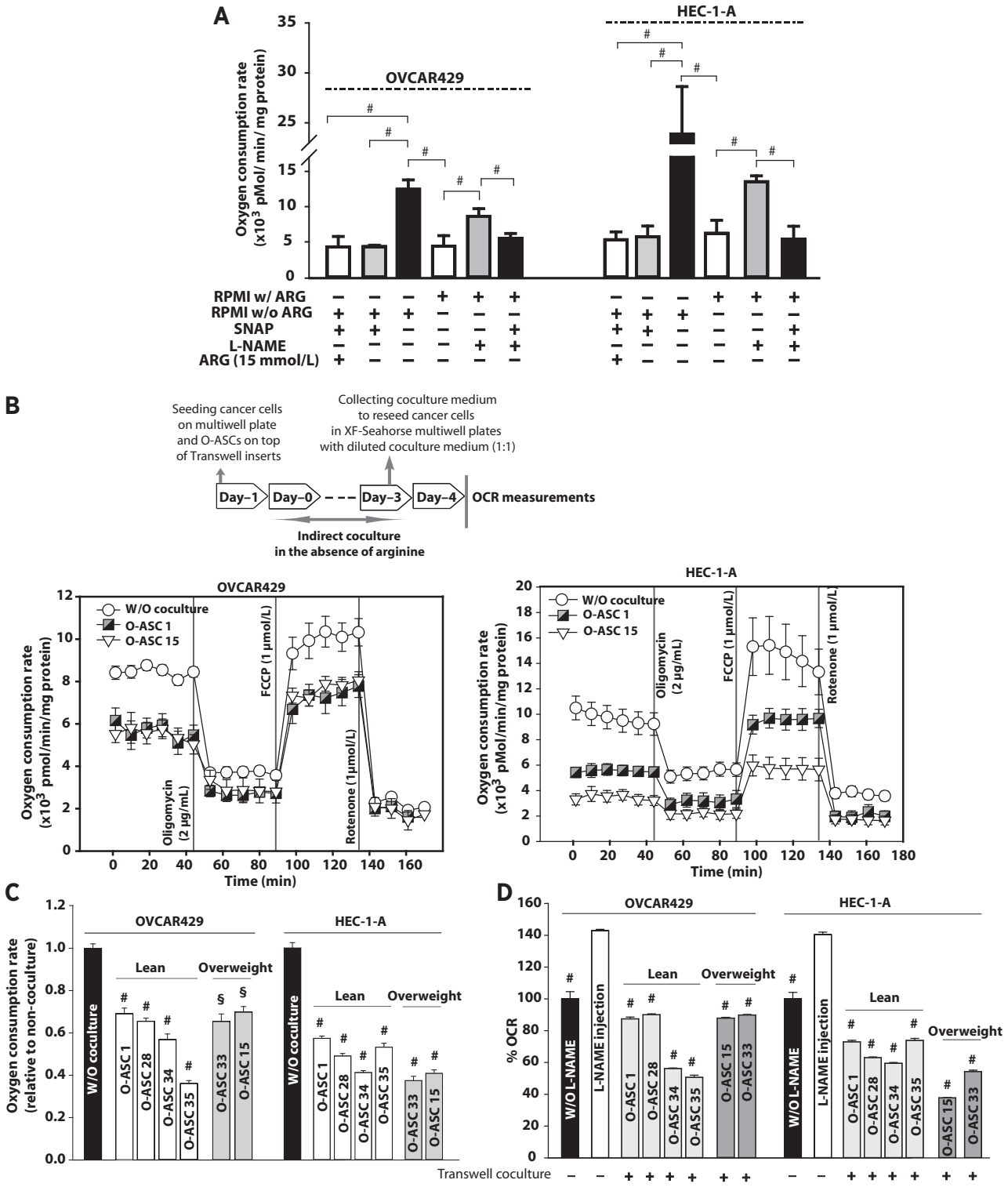

Figure 5.

O-ASCs modulate cancer cells' mitochondrial bioenergetics. A, cancer cells were seeded in XF Seahorse multiwell plates and were incubated overnight until cells were attached to the surface. Cancer cells OCR levels were measured after treating cancer cells with SNAP (100 nmol/L), exogenous L-arginine (15 mmol/L), and L-NAME (10 mmol/L) for 3 hours before assay execution. B and C, cancer cells were reseeded in XF-seahorse multiwell plates after 3 days of transwell coculture with O-ASCs. The media of coculture did not include arginine and cells were reseeded with diluted (1:1) coculture media. Oligomycin (2 µg/mL), FCCP (1 µmol/L), and rotenone (1 µmol/L) were injected through the cartridge ports. Cells were lysed and quantified for their protein contents and used for normalization of data. D, cancer cells from transwell cocultures were injected with L-NAME (20 mmol/L) in the cartridge. Data are expressed as mean ± SE; $n > 6$. *, $P < 0.05$; §, $P < 0.01$; and #, $P < 0.001$. All pairwise multiple comparisons were analyzed by the Bonferroni test. The Dunnett method was implemented to compare multiple groups versus a control group.

Published OnlineFirst November 25, 2014; DOI: 10.1158/0008-5472.CAN-14-1337

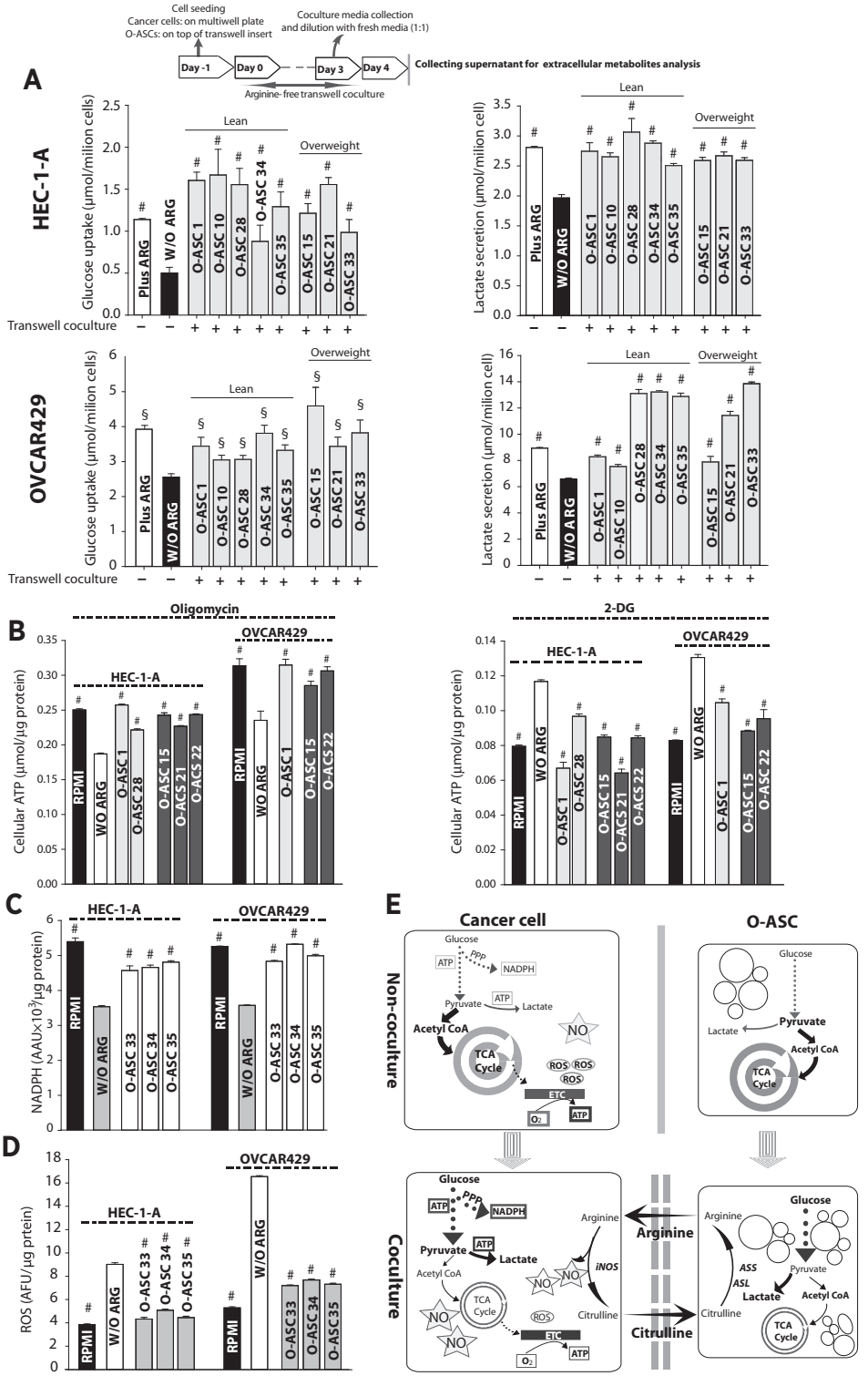

Figure 6.
O-ASCs regulate ovarian cancer and endometrial cancer cells metabolism via NO pathways. OVCAR429 and HEC-1-A were indirectly cocultured with O-ASCs for 3 days. The control cells from monoculture were seeded at the same time as cells with transwell coculture. Similar culture methods were used for cells in coculture and monocultures. The culture media were RPMI-1640 without arginine during 3 days of indirect coculture. Cocultured media were collected on the third day and diluted (1:1) with fresh RPMI (without arginine). Cancer cells were incubated with diluted media for 24 hours before supernatant collection. Collected samples were analyzed for their extracellular metabolites content. A, glucose uptake and lactate secretion of cancer cells. B, cancer cells from transwell cocultures of O-ASCs were reseeded with diluted media in 96-well plates. The cells were incubated at 37°C overnight until cells are attached to the surface. Oligomycin (2 μg/μL) or 2-DG (100 mmol/L) was added 3 hours before assay execution. Glycolysis and mitochondrial ATP contribution were assessed with these inhibitors. Cancer cells without coculture and without arginine were used as control. Cancer cells from transwell cocultures of O-ASCs were reseeded and assessed for NADPH (C) and ROS (D) levels. E, schematic illustrates reciprocal interaction between cancer cells and O-ASCs before and after coculture. Data are expressed for each cell type as the mean ± SE; $n > 3$. *, $P < 0.05$; §, $P < 0.01$; and #, $P < 0.001$. The Dunnett method was used to compare multiple groups versus a control group.

cocultures, we measured glycolytic and mitochondrial ATP contribution using oligomycin (inhibits electron transport chain) and 2-DG (inhibits glycolysis), respectively. Consistent with the above results, we found that O-ASCs increased the glycolytic ATP generation but decreased the mitochondrial ATP generation in both ovarian cancer and endometrial cancer cells (Fig. 6B). Because cancer cells may divert increased glucose to the pentose phosphate pathway for NADPH generation to decrease ROS, we next measured NADPH. We found that NO increased NADPH synthesis (Fig. 6C) and decreased ROS (Fig. 6D). Notably, O-ASCs

Published OnlineFirst November 25, 2014; DOI: 10.1158/0008-5472.CAN-14-1337

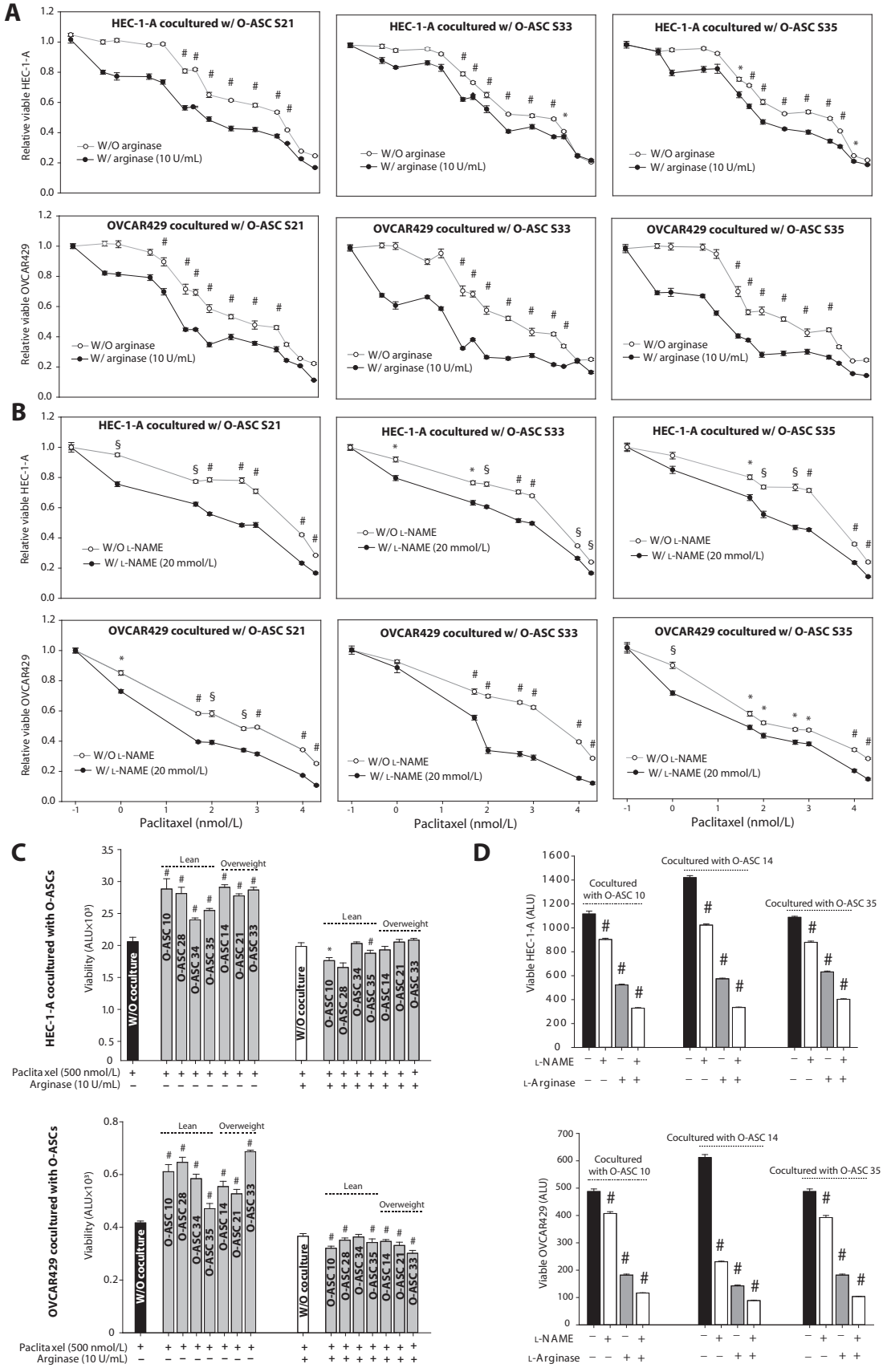

Published OnlineFirst November 25, 2014; DOI: 10.1158/0008-5472.CAN-14-1337

increased NADPH and reduced ROS in cocultures under arginine-deprivation conditions. These results substantiate the role of O-ASC–secreted factors that modulate NO homeostasis in cancer cells and thereby upregulate glycolysis and reduce oxidative stress (30).

O-ASCs induce chemoresistance of cancer cells

The above results show that O-ASCs secrete factors that modulate NO homeostasis and increases cancer cells' proliferation and alters cancer metabolism. We recently showed that O-ASCs induce chemoresistance in cancer cells (8). Here, we asked whether this O-ASC–mediated chemoresistance can be deregulated by disrupting NO homeostasis. We added L-arginase in direct-contact cocultures of O-ASCs and cancer cells. The L-arginase depletes any secreted arginine by O-ASCs and blocks NO synthesis in cancer cells. Remarkably, we found that addition of L-arginase to direct-contact cocultures increased chemosensitivity of paclitaxel in cancer cells (Fig. 7A). Furthermore, addition of L-NAME in direct-contact cocultures also had similar effect and increased sensitivity of paclitaxel in cancer cells (Fig. 7B). Similar results were obtained with additional O-ASCs patient samples treated with L-arginase at 10 U/mL (Fig. 7C). To confirm the involvement of NO in increasing resistance of cancer cells to paclitaxel, we added SNAP in cancer cells cultured with either L-arginase or L-NAME in the presence and absence of paclitaxel (Supplementary Fig. S5). We found that SNAP decreased sensitivity of cancer cells to paclitaxel, thus corroborating our previous results. We further evaluated whether combinatorial addition of L-NAME and L-arginase will have synergistic effect in disrupting the NO-mediated communication between O-ASCs and cancer. Indeed, adding both L-NAME and L-arginase significantly reduced the cell viability in cancer cells in cocultures with O-ASCs (Fig. 7D). These results suggest that a combined approach of targeting secreted arginine through L-arginase, along with targeting microenvironment-secreted factors induced increased NO synthesis in cancer cells using L-NAME, may be a viable therapeutic approach for targeting ovarian cancers and endometrial cancers.

Discussion

Here, our results revealed mechanism behind the interaction between O-ASCs and cancer cells. We found that O-ASCs promoted the growth of both ovarian cancer and endometrial cancer cells through NO. Interestingly, O-ASCs secrete arginine under arginine-deprivation conditions and this secreted arginine was uptaken by cancer cells, thereby increases NO synthesis and cancer cells' growth rate. Arginine depletion is currently used as a therapy for melanoma and hepatocellular carcinoma (31, 32). We showed that when O-ASC–secreted arginine is depleted (using L-arginase) or when O-ASC–secreted factors induced increased NO synthesis in cancer cells is inhibited (using L-NAME), there is a decline in the growth rate of both ovarian cancer and endometrial cancer cells. It was previously reported by our group that ovarian cancer cells secrete considerable amount of citrulline, thereby indicating high NOS activity and arginine utilization (33). Here, our data showed that ovarian cancer and endometrial cancer cells use arginine produced by O-ASCs and generate citrulline. Remarkably, citrulline secreted by cancer cells increased the adipogenesis of O-ASCs. Thus, our findings propose a previously unexplored metabolic coupling between cancer cells and O-ASCs.

Recent studies proposed metabolic-symbiosis as a reciprocal coupling between cancer cells and its microenvironment (34). In these studies, tumor microenvironment cells, mainly cancer associated fibroblasts, were shown to be in catabolic state, thus generating energy-rich metabolites (such as lactate, glutamine, fatty acids, and other amino acids) that are then used by cancer cells' mitochondria for OXPHOS (35). However, our findings show that O-ASCs rescue cancer cells loss of growth under arginine-deprivation conditions, by secreting arginine for cell growth/biosynthesis but not for energetic needs. Arginine utilization for NO as a signaling molecule dominated other roles of arginine in cellular functions. As seen in Fig. 3G, growth of cancer cells decreased significantly when arginine was excluded from media and SNAP compensated this decrease induced by arginine deprivation. These results emphasize the crucial role of arginine in NO synthesis.

In contrast with Warburg effect, recent data suggest that cancer cells have healthy mitochondria; however, they have upregulated glycolysis (36). Interestingly, our data suggest that O-ASCs promoted glycolysis in cancer cells by elevating NO synthesis, which has been shown to have inhibitory effects on enzymes involved in mitochondrial respiration. Previous studies showed that NO affects glycolysis through s-nitrosylation of hexokinase (37). Hexokinase converts glucose to glucose-6-phosphate in the first step of glycolysis and is highly expressed in cancer cells (38). Low concentrations of NO (below 100 nmol/L) induce hypoxia-inducible factor 1-α (HIF1α) expression and mimics low oxygen conditions (39). HIF1α, a key regulator of hypoxia, switches energy metabolism from oxidative phosphorylation to glycolysis by regulating glucose transporter-1 (GLUT-1), lactate dehydrogenase (LDH), and pyruvate dehydrogenase (PDH) expression (40). We here showed that O-ASCs positively regulate the Warburg effect by modulating the NO homeostasis. O-ASC–secreted arginine increased NO synthesis in cancer cells that reprogrammed cancer cells by increasing glycolysis and reducing mitochondrial ATP generation. Treating cancer cells with arginine-depleted media showed that reducing NO levels reduced glucose and pyruvate consumption of cells as well as their lactate secretion levels. Remarkably, O-ASCs interaction with cancer cells compensated the reduced levels of metabolites. Consistent with our hypothesis, we found that O-ASCs increased glucose uptake and lactate secretion of cancer cells under arginine-deprivation conditions. O-ASC–modulated ovarian and endometrial cancer cell metabolism via arginine secretion that when uptaken by cancer

Figure 7.

O-ASCs induce chemoresistance in cancer cells. Stably luciferase transfected cancer cells and O-ASCs were seeded in 96-well plate and cocultured in direct contact for 48 hours before their exposure to different concentrations of paclitaxel along with L-arginase (10 U/mL; A) or L-NAME (20 mmol/L; B).Viability of cancer cells was assessed by addition of luciferin (150 μg/mL) for 1 hour and the corresponding luminescence was measured. C, more patient samples were incorporated to illustrate the increased chemoresistance of cancer cells when directly cocultured with O-ASCs and L-arginase (10 U/mL). D, cancer cells and O-ASCs (ratio 1:3) were directly cocultured in 96-well plates and treated with L-arginase, L-NAME, or their combination for 3 days. Data are expressed for each cell type as the mean ± SE; $n > 6$. *, $P < 0.05$; §, $P < 0.01$; and #, $P < 0.001$. The curves are compared at each point using the Bonferroni test. The Dunnett method was used to compare multiple groups versus a control group (C).

Published OnlineFirst November 25, 2014; DOI: 10.1158/0008-5472.CAN-14-1337

cells increased NO in these cells. Figure 6E summarizes our results obtained on metabolic coupling between O-ASCs and cancer cells. On the basis of our results, "NO homeostasis" could be a key player in regulating reciprocal communication between O-ASCs and gynecologic cancer cells. The reciprocal communication was observed between cancer cells and O-ASCs, where cancer cells were found to increase glucose metabolism and adipogenesis in O-ASCs.

NO has been known to influence respiration rates of cancer cells by targeting mitochondrial complexes, complex I and IV (41,42). Previous studies carried out primarily in liver cells showed that NO regulates mitochondrial respiration by targeting terminal enzyme of electron transport chain, cytochrome *c* oxidase by competing with oxygen (43). Inhibition of complex IV is rapid (milliseconds), reversible, and occurs at low NO concentrations (nmol/L), whereas inhibition of complex I occurs after a constant exposure of higher NO concentrations (44, 45). NO's inhibition of mitochondrial respiration in cancer cells shifts them from oxidative phosphorylation to glycolysis. Here, we showed that arginine deprivation decreases NO, thereby increases OCR of OVCAR429 and HEC-1-A cells (Fig. 5A). O-ASCs decreased OCR of cancer cells by secreting arginine, a substrate for NO synthesis under arginine-deprivation conditions. We demonstrated that NO can shift source of ATP generation in cancer cells cocultured with O-ASCs by increasing glycolytic ATP production and concomitantly decrease mitochondrial contribution toward ATP production (Fig. 6B).

Recent studies have shown that O-ASCs induce chemoresistance in cancer cells (46). Multiple lines of evidence support the link between NO and chemoresistance (47–50). Herein, we show that O-ASCs regulate cancer cells' response to chemo-drugs through the NO pathway. Inhibition of NO synthesis, sensitized cancer cells cocultured with O-ASCs to paclitaxel (Fig. 7A–C). Furthermore, our studies suggest that combinatorial therapy of depleting arginine using L-arginase, along with inhibiting NO using L-NAME, could disrupt the communication between O-ASCs and cancer cells. Our data present mechanistic insights into O-ASC–mediated metabolic reprogramming in cancer cells and also reciprocal modulation of O-ASCs adipogenesis by cancer cells. Future studies are needed to investigate the therapeutic strategies targeting the impact of O-ASC on cancer initiation and progression. The detailed analysis of altered NO metabolism of cancer cells in the presence of O-ASCs will shed light on the molecular pathways regulated by O-ASCs and thus allow development of targeted therapies linking signaling, transcriptional changes with metabolic signatures linking obesity with cancer.

Disclosure of Potential Conflicts of Interest

No potential conflicts of interest were disclosed.

Authors' Contributions

Conception and design: B. Salimian Rizi, C. Caneba, D. Nagrath
Development of methodology: B. Salimian Rizi, D. Nagrath
Acquisition of data (provided animals, acquired and managed patients, provided facilities, etc.): B. Salimian Rizi, A.W. Nabiyar, X. Liu, K. Chen, D. Nagrath
Analysis and interpretation of data (e.g., statistical analysis, biostatistics, computational analysis): B. Salimian Rizi, A.W. Nabiyar, A. Klopp, D. Nagrath
Writing, review, and/or revision of the manuscript: B. Salimian Rizi, A. Klopp, D. Nagrath
Administrative, technical, or material support (i.e., reporting or organizing data, constructing databases): B. Salimian Rizi, A. Nowicka
Study supervision: B. Salimian Rizi, D. Nagrath
Other (discussions): A. Nowicka
Other (nitric oxide, nitrite, and nitrates measurements, using Ozone chemiluminescence technology and provision of analyzer and test methodology for running samples): A.W. Nabiyar

Grant Support

This work was made possible, in part, through support from the Ken Kennedy Institute for Information Technology at Rice University to D. Nagrath under the Collaborative Advances in Biomedical Computing 2011 seed funding program supported by the John and Ann Doerr Fund for the Computational Biomedicine.

The costs of publication of this article were defrayed in part by the payment of page charges. This article must therefore be hereby marked advertisement in accordance with 18 U.S.C. Section 1734 solely to indicate this fact.

Received May 6, 2014; revised October 6, 2014; accepted October 24, 2014; published OnlineFirst November 25, 2014.

References

1. Nieman KM, Kenny HA, Penicka CV, Ladanyi A, Buell-Gutbrod R, Zillhardt MR, et al. Adipocytes promote ovarian cancer metastasis and provide energy for rapid tumor growth. Nat Med 2011;17:1498–503.
2. Nieman KM, Romero IL, Van Houten B, Lengyel E. Adipose tissue and adipocytes support tumorigenesis and metastasis. Biochim Biophys Acta 2013;1831:1533–41.
3. Hu J, Liu Z, Wang X. Does TP53 mutation promote ovarian cancer metastasis to omentum by regulating lipid metabolism? Med Hypotheses 2013;81:515–20.
4. Park YM, Yoo SH, Kim SH. Adipose-derived stem cells induced EMT-like changes in H358 lung cancer cells. Anticancer Res 2013; 33:4421–30.
5. Dirat B, Bochet L, Dabek M, Daviaud D, Dauvillier S, Majed B, et al. Cancer-associated adipocytes exhibit an activated phenotype and contribute to breast cancer invasion. Cancer Res 2011;71:2455–65.
6. Kidd S, Spaeth E, Watson K, Burks J, Lu H, Klopp A, et al. Origins of the tumor microenvironment: quantitative assessment of adipose-derived and bone marrow-derived stroma. PLoS ONE 2012;7:e30563.
7. Behan JW, Yun JP, Proektor MP, Ehsanipour EA, Arutyunyan A, Moses AS, et al. Adipocytes impair leukemia treatment in mice. Cancer Res 2009;69:7867–74.
8. Nowicka A, Marini FC, Solley TN, Elizondo PB, Zhang Y, Sharp HJ, et al. Human omental-derived adipose stem cells increase ovarian cancer proliferation, migration, and chemoresistance. PLoS ONE 2013;8:e81859.
9. Klopp AH, Zhang Y, Solley T, Amaya-Manzanares F, Marini F, Andreeff M, et al. Omental adipose tissue-derived stromal cells promote vascularization and growth of endometrial tumors. Clin Cancer Res 2012;18: 771–82.
10. Sanuphan A, Chunhacha P, Pongrakhananon V, Chanvorachote P. Long-term nitric oxide exposure enhances lung cancer cell migration. Biomed Res Int 2013;2013:186972.
11. Clark R, Krishnan V, Schoof M, Rodriguez I, Theriault B, Chekmareva M, et al. Milky spots promote ovarian cancer metastatic colonization of peritoneal adipose in experimental models. Am J Pathol 2013;183:576–91.
12. Quail DF, Joyce JA. Microenvironmental regulation of tumor progression and metastasis. Nat Med 2013;19:1423–37.
13. Heller A. The need for monitoring the actual nitric oxide concentration in tumors. Bioanal Rev 2009;1:3–6.
14. Xu W, Liu LZ, Loizidou M, Ahmed M, Charles IG. The role of nitric oxide in cancer. Cell Res 2002;12:311–20.
15. Muntane J, la Mata MD. Nitric oxide and cancer. World J Hepatol 2010; 2:337–44.

Published OnlineFirst November 25, 2014; DOI: 10.1158/0008-5472.CAN-14-1337

16. Elizalde M, Ryden M, van Harmelen V, Eneroth P, Gyllenhammar H, Holm C, et al. Expression of nitric oxide synthases in subcutaneous adipose tissue of nonobese and obese humans. J Lipid Res 2000;41:1244–51.
17. Ryden M, Elizalde M, van Harmelen V, Ohlund A, Hoffstedt J, Bringman S, et al. Increased expression of eNOS protein in omental versus subcutaneous adipose tissue in obese human subjects. Int J Obes Relat Metab Disord 2001;25:811–5.
18. Thomsen LL, Lawton FG, Knowles RG, Beesley JE, Riveros-Moreno V, Moncada S. Nitric oxide synthase activity in human gynecological cancer. Cancer Res 1994;54:1352–4.
19. Thomsen LL, Miles DW, Happerfield L, Bobrow LG, Knowles RG, Moncada S. Nitric oxide synthase activity in human breast cancer. Br J Cancer 1995; 72:41–4.
20. Grisham MB, Jourd'Heuil D, Wink DA. Nitric oxide. I. Physiological chemistry of nitric oxide and its metabolites:implications in inflammation. Am J Physiol 1999;276:G315–21.
21. Choudhari SK, Chaudhary M, Bagde S, Gadbail AR, Joshi V. Nitric oxide and cancer: a review. World J Surg Oncol 2013;11:118.
22. Harada K, Supriatno, Kawaguchi S, Tomitaro O, Yoshida H, Sato M. Overexpression of iNOS gene suppresses the tumorigenicity and metastasis of oral cancer cells. In Vivo 2004;18:449–55.
23. Shang ZJ, Li JR, Li ZB. Effects of exogenous nitric oxide on oral squamous cell carcinoma: an *in vitro* study. J Oral Maxillofac Surg 2002;60:905–10; discussion 10–1.
24. Dang CV. Role of aerobic glycolysis in genetically engineered mouse models of cancer. BMC Biol 2013;11:3.
25. Barron DA, Rowley DR. The reactive stroma microenvironment and prostate cancer progression. Endocr Relat Cancer 2012;19:R187–204.
26. Sottile V, Seuwen K. A high-capacity screen for adipogenic differentiation. Anal Biochem 2001;293:124–8.
27. Rhodes DR, Kalyana-Sundaram S, Mahavisno V, Varambally R, Yu J, Briggs BB, et al. Oncomine 3.0: genes, pathways, and networks in a collection of 18,000 cancer gene expression profiles. Neoplasia 2007;9: 166–80.
28. Kaasik A, Minajeva A, De Sousa E, Ventura-Clapier R, Veksler V. Nitric oxide inhibits cardiac energy production via inhibition of mitochondrial creatine kinase. FEBS Lett 1999;444:75–7.
29. Whitaker-Menezes D, Martinez-Outschoorn UE, Lin Z, Ertel A, Flomenberg N, Witkiewicz AK, et al. Evidence for a stromal-epithelial "lactate shuttle" in human tumors: MCT4 is a marker of oxidative stress in cancer-associated fibroblasts. Cell Cycle 2011;10:1772–83.
30. Caneba CA, Yang L, Baddour J, Curtis R, Win J, Hartig S, et al. Nitric oxide is a positive regulator of the Warburg effect in ovarian cancer cells. Cell Death Dis 2014;5:e1302.
31. Yoon JK, Frankel AE, Feun LG, Ekmekcioglu S, Kim KB. Arginine deprivation therapy for malignant melanoma. Clin Pharmacol 2013;5:11–9.
32. Cheng PN, Lam TL, Lam WM, Tsui SM, Cheng AW, Lo WH, et al. Pegylated recombinant human arginase (rhArg-peg5,000mw) inhibits the *in vitro* and *in vivo* proliferation of human hepatocellular carcinoma through arginine depletion. Cancer Res 2007;67:309–17.
33. Caneba CA, Bellance N, Yang L, Pabst L, Nagrath D. Pyruvate uptake is increased in highly invasive ovarian cancer cells under anoikis conditions for anaplerosis, mitochondrial function, and migration. Am J Physiol Endocrinol Metab 2012;303:E1036–52.
34. Bonuccelli G, Tsirigos A, Whitaker-Menezes D, Pavlides S, Pestell RG, Chiavarina B, et al. Ketones and lactate "fuel" tumor growth and metastasis: evidence that epithelial cancer cells use oxidative mitochondrial metabolism. Cell Cycle 2010;9:3506–14.
35. Sotgia F, Martinez-Outschoorn UE, Lisanti MP. Cancer metabolism: new validated targets for drug discovery. Oncotarget 2013;4:1309–16.
36. Yang L, Moss T, Mangala LS, Marini J, Zhao H, Wahlig S, et al. Metabolic shifts toward glutamine regulate tumor growth, invasion and bioenergetics in ovarian cancer. Mol Sys Biol 2014;10:728.
37. Doulias PT, Tenopoulou M, Greene JL, Raju K, Ischiropoulos H. Nitric oxide regulates mitochondrial fatty acid metabolism through reversible protein S-nitrosylation. Sci Signal 2013;6:rs1.
38. Smith TA. Mammalian hexokinases and their abnormal expression in cancer. Br J Biomed Sci 2000;57:170–8.
39. Chowdhury R, Godoy LC, Thiantanawat A, Trudel LJ, Deen WM, Wogan GN. Nitric oxide produced endogenously is responsible for hypoxia-induced HIF-1alpha stabilization in colon carcinoma cells. Chem Res Toxicol 2012;25:2194–202.
40. Lum JJ, Bui T, Gruber M, Gordan JD, DeBerardinis RJ, Covello KL, et al. The transcription factor HIF-1alpha plays a critical role in the growth factor-dependent regulation of both aerobic and anaerobic glycolysis. Genes Dev 2007;21:1037–49.
41. Sarti P, Arese M, Forte E, Giuffre A, Mastronicola D. Mitochondria and nitric oxide: chemistry and pathophysiology. Adv Exp Med Biol 2012;942: 75–92.
42. Ball KA, Nelson AW, Foster DG, Poyton RO. Nitric oxide produced by cytochrome c oxidase helps stabilize HIF-1alpha in hypoxic mammalian cells. Biochem Biophys Res Commun 2012;420:727–32.
43. Brookes PS, Kraus DW, Shiva S, Doeller JE, Barone MC, Patel RP, et al. Control of mitochondrial respiration by NO*, effects of low oxygen and respiratory state. J Biol Chem 2003;278:31603–9.
44. Sen S, Kawahara B, Chaudhuri G. Mitochondrial-associated nitric oxide synthase activity inhibits cytochrome c oxidase: implications for breast cancer. Free Radic Biol Med 2013;57:210–20.
45. Wang F, Zhang R, Xia T, Hsu E, Cai Y, Gu Z, et al. Inhibitory effects of nitric oxide on invasion of human cancer cells. Cancer Lett 2007;257: 274–82.
46. Moreno-Smith M, Halder JB, Meltzer PS, Gonda TA, Mangala LS, Rupaimoole R, et al. ATP11B mediates platinum resistance in ovarian cancer. J Clin Invest 2013;123:2119–30.
47. Muerkoster S, Wegehenkel K, Arlt A, Witt M, Sipos B, Kruse ML, et al. Tumor stroma interactions induce chemoresistance in pancreatic ductal carcinoma cells involving increased secretion and paracrine effects of nitric oxide and interleukin-1beta. Cancer Res 2004;64: 1331–7.
48. Godoy LC, Anderson CT, Chowdhury R, Trudel LJ, Wogan GN. Endogenously produced nitric oxide mitigates sensitivity of melanoma cells to cisplatin. Proc Natl Acad Sci U S A 2012;109:20373–8.
49. Muerkoster SS, Lust J, Arlt A, Hasler R, Witt M, Sebens T, et al. Acquired chemoresistance in pancreatic carcinoma cells: induced secretion of IL-1beta and NO lead to inactivation of caspases. Oncogene 2006;25: 3973–81.
50. Yang DI, Yin JH, Mishra S, Mishra R, Hsu CY. NO-mediated chemoresistance in C6 glioma cells. Ann N Y Acad Sci 2002;962:8–17.

Published OnlineFirst November 25, 2014; DOI: 10.1158/0008-5472.CAN-14-1337

Cancer Research

Nitric Oxide Mediates Metabolic Coupling of Omentum-Derived Adipose Stroma to Ovarian and Endometrial Cancer Cells

Bahar Salimian Rizi, Christine Caneba, Aleksandra Nowicka, et al.

Cancer Res Published OnlineFirst November 25, 2014.